Separation Science and Technology
Publication details, including instructions for authors and subscription information:
http://www.informaworld.com/smpp/title~content=t713708471

A General Plate-Height Expression for Open Tubular Column Chromatography

T. W. Smuts[a]; K. De Clerk[a]; Victor Pretorius[a]
[a] C.S.I.R. Research Unit Department of Physical, Theoretical Chemistry University of Pretoria Pretoria, Republic of South Africa

To cite this Article Smuts, T. W. , De Clerk, K. and Pretorius, Victor(1968) 'A General Plate-Height Expression for Open Tubular Column Chromatography', Separation Science and Technology, 3: 1, 43 — 65
To link to this Article: DOI: 10.1080/01496396808052206
URL: http://dx.doi.org/10.1080/01496396808052206

SEPARATION SCIENCE, 3(1), pp. 43–65, Feb., 1968

A General Plate-Height Expression for Open Tubular Column Chromatography

T. W. SMUTS, K. DE CLERK, and VICTOR PRETORIUS
C.S.I.R. RESEARCH UNIT
DEPARTMENT OF PHYSICAL AND THEORETICAL CHEMISTRY
UNIVERSITY OF PRETORIA
PRETORIA, REPUBLIC OF SOUTH AFRICA

Summary

The plate-height behavior of open tubular columns, for both gases and liquids, has been studied fundamentally in the turbulent flow region. Appriate analytical expressions have been established on the basis of a purely phenomenological description of turbulent flow dynamics. It has been shown that under these flow conditions, the plate height decreases with increasing Reynolds number and that, most significantly, this decrease is strongly dependent on the mass distribution coefficient.

INTRODUCTION

It has been suggested (*1–3*) that by inducing "turbulence" in the mobile phase of chromatographic systems the efficiency may, under suitable circumstances, be improved and the separation time reduced. Pretorius and Smuts (*1*) have made a preliminary attempt to evaluate the broad trends of chromatographic behavior in the turbulent flow region on theoretical grounds using empirical data on velocity profile and dispersion coefficients. Giddings (*4*) has discussed the characteristics of turbulent flow qualitatively and subsequently (*2*) also presented some experimental data on the performance of columns operating under turbulent flow conditions. From none of these investigations, however, do the merits of turbulent flow chromatographing emerge unequivocably and there is a need for a more exhaustive analysis of the technique. As a first

step the present study has been undertaken to establish a plate-height expression covering both the laminar and turbulent flow regions in open tubular columns and also to discuss those aspects of turbulent flow which have a bearing on chromatography.

It has been shown (*1,5*) that a general expression for the plate height of open tubular columns as measured at the column outlet is

$$H = \left(\frac{2D_1}{\bar{u}} + \frac{2I_1\bar{u}_o r_t^2}{D'_{ro}}\right) f_m + C_s\bar{u}_o f_s \tag{1}$$

$$= H_M(x) f_m + C_s\bar{u}_o f_s$$

where

$$I_1 = \int_o^{r_t} \frac{dr}{2r\psi(r)}\left[\Phi(r) - \frac{1}{1+k}\left(\frac{r}{r_t}\right)^2\right]^2$$

$$= \frac{(I_{11} - I_{12} + I_{13}) + 2(I_{11} - I_{12})k + I_{11}k^2}{(1+k)^2} \tag{2}$$

and $\Phi(r)$ of the form

$$\Phi(r) = \int_o^r \frac{2r'\phi(r')\,dr'}{r_t} \tag{3}$$

$\psi(r)$ is a function which relates the radial dispersion coefficient $D(r)$ at radial position r to a reference value D'_r by the expression

$$D_r(r) = D'_r\psi(r) \tag{4}$$

$\phi(r)$ is a similar function defined by

$$u(r) = \bar{u}\phi(r) \tag{5}$$

where the mean velocity $\bar{u}$ is chosen as reference. The term dispersion coefficient is used in a general sense. It includes, additively, all the dispersion coefficients defined by phenomenological Fickian laws for the various mass-transport processes. In the present context it is therefore the sum of the molecular and eddy diffusion coefficients. D_1 is the longitudinal dispersion coefficient. A previous investigation of band dispersion in turbulent flow by Taylor (*6*) shows, in a somewhat different context, that of the two terms included in the parentheses in Eq. (1) the first is about 0.01 times as large as the second. This result has also been confirmed by de Clerk (*7*) and this term can be neglected in the ex-

pression for H for the turbulent flow region. C_s is the coefficient of $\bar{u}(x)$ in the term representing the contribution of the plate height of resistance to lateral mass transfer in the stationary phase. The quantities f_m and f_s are familiar (8,9) functions that correct for the compressibility of the mobile phase. These functions are identical for both the laminar and turbulent flow regions, since the flow dynamics does not enter in their derivation (5). To make Eq. (1) valid for incompressible fluids, it will be assumed that f_m and f_s are equal to unity for such fluids. In general therefore

$$f_m = \frac{9(p^4-1)(p^2-1)}{8(p^3-1)^2} \text{ (compressible ideal gases)} \qquad (6)$$

$$= 1 \text{ (incompressible fluids)}$$

$$f_s = \frac{3}{2}\frac{(p^2-1)}{(p^3-1)} \text{ (compressible ideal gases)} \qquad (7)$$

$$= 1 \text{ (incompressible fluids)}$$

Equation (1) may now be regarded as a general form of the well-known Golay expression in that it is valid for any type of flow that can be characterized by suitable functions $\phi(r)$ and $\psi(r)$. Thus for laminar flow

$$\phi(r) = 2\left[1 - \left(\frac{r}{r_t}\right)^2\right] \qquad (8)$$

and

$$D(r) = D_m \qquad (9)$$

Evaluation of I_1 via Eqs. (2), (8), and (9) reduces Eq. (1) to the Golay equation, viz.,

$$H = \frac{2D_{mo}}{\bar{u}_o} f_m + \left[\frac{1 + 6k + 11k^2}{24(1+k)^2}\right]\frac{r_t^2 \bar{u}_o}{D_{mo}} f_m + C_s \bar{u}_o f_s \qquad (10)$$

To evaluate the plate height for the turbulent flow region from Eq. (1), it is clearly necessary that the functions $\psi(r)$ and $\phi(r)$ must be known for this flow region; the complexity of the turbulent flow dynamics recessitates a phenomenological approach.

PHENOMENOLOGICAL DESCRIPTION OF TURBULENT FLOW

Turbulent flow in open tubes is characterized by violet random movement (*10–12*) of macroscopic fluid elements. The magnitude

of the distances over which these movements occur varies greatly (*10,11*) but the upper limit is similar to the tube diameter (*10,12*). Those random movements, often referred to as eddies (*10,11,14*), are superimposed on axial flow in the conduit. The turbulence in the fluid manifests itself in several ways. The fluid appears to be more viscous in that a smaller increase in the average linear flow velocity for a fixed increment in the pressure drop across the column is observed in the turbulent than in the laminar flow region. Furthermore, heat- and mass-transfer rates are much larger in the turbulent than in the laminar flow region. All these properties of turbulent flow can be satisfactorily predicted by a phenomenological description. This would merely correlate the observed experimental measurements, without necessarily further speculating about the origin of the observed phenomenon in terms of more fundamental concepts.

For the purpose of quantitatively describing ψ and ϕ by means of phenomenological variables, it is necessary to consider the flow velocity at which turbulence sets in. This flow velocity cannot, in principle, be predicted by a consideration of the normal hydrodynamic relations such as the Navier–Stokes equation (*15*). Although solutions of those equations are valid at all flow velocities, flows which are predicted are, however, not necessarily stable in real situations. It is found that for real flows above a critical flow velocity, small perturbations of the flow patterns are increased and turbulence sets in. It is more general to refer to this flow region as unstable since in the absence of perturbation the flow dynamics will remain laminar (*14*). Similarly perturbations in the flow system at flow velocities below the critical may cause deviations from streamline flow (*11*), but there will be a tendency for these perturbations to be damped out. The fundamental cause of the observed instability has not been explained satisfactorily (*11,15*). It has, however, been demonstrated that this critical flow velocity can be correlated by the well-known dimensionless group, viz., the Reynolds number, $\mathrm{Re} = 2r_t\bar{u}/\nu$ (*11,15,16*). Experimental observation has indicated that this critical value of the Reynolds number is about 2100 (*11,15,16*).

The random nature of turbulent flow necessitates statistical methods for its description (*17,18*). Consider therefore a macroscopic fluid element, small enough to allow its constituent molecules to move coherently together. This element moves about

randomly and the following average quantities serve to describe its movement at any point in real space:

$$u' = \bar{u}' + u''$$
$$v' = \bar{v}' + v''$$
$$w' = \bar{w}' + w''$$

where $\bar{u}'$ is the component of the average velocity in the axial direction and u'' the component of the turbulent fluctuation velocity in the same direction. $\bar{v}'$, $\bar{w}'$, v'', and w'' are similar quantities for the y and z axes in a rectangular cartesian representation. For an open tube $\bar{v}' = \bar{w}' = 0$, but the associated turbulent velocity fluctuations are, however, not zero. For the present study it is sufficient to consider the behavior of the representative fluid element only in the lateral direction.

Prandtl (*19*) and others (*20,21*) have suggested that the movement of the macroscopic fluid elements can be considered to be very similar to that of gas molecules. This analogy has led to the introduction of a number of concepts for the description of turbulence which are similar to those employed in the theory of gas kinetics. A characteristic length, analogous to the mean free path length concept of gas kinetics, is one of these. This quantity is known as the mixing length and is defined as that distance which a fluid element must move with its initial mean velocity in the transverse direction until its flow velocity in the axial direction differs from that of the surrounding fluid elements by an amount equal to the mean transverse fluctuation in the turbulent velocity (*13, 19*), i.e.,

$$|\bar{v}''| = l \left| \frac{d\bar{u}(y)}{dy} \right| \tag{11}$$

where l is the mixing length. The present analogy can now be taken to its logical conclusion by the introduction of momentum and mass-transfer laws similar to those well known in gas kinetics. Thus, following arguments analogous to the derivation of an expression for the shear stress present in gas flow, it is found that (*10,11,22*)

$$\tau_t' = -\rho'(l)^2 \left| \frac{d\bar{u}(y)}{dy} \right| \frac{d\bar{u}}{dy} = \rho' \epsilon' \frac{d\bar{u}}{dy} \tag{12}$$

In analogy to the phenomenological relation between τ', $d\bar{u}/dy$,

and the kinematic viscosity coefficient (*10,22*), viz.,

$$\tau' = -\rho' \nu \frac{d\bar{u}}{dy} \tag{13}$$

ϵ' can therefore be regarded as a virtual kinematic viscosity coefficient (*10,11,13*). By means of dimensional arguments, von Karman (*23*) has shown that for eddies at a distance from the wall

$$l = \kappa \left| \frac{d\bar{u}/dy}{d^2\bar{u}/dy^2} \right| \tag{14}$$

where κ is an empirical constant for all turbulent flows. From Eqs. (12–14) it thus follows that

$$\epsilon' = \kappa^2 \frac{(d\bar{u}/dy)^3}{(d^2\bar{u}/d^2y)^2} \tag{15}$$

In the region very close to the wall, Eq. (15) is not valid. A number of expressions have been proposed (*24–26*) for ϵ' in this region—again from dimensional arguments. These expressions will not be given here, but they are shown in Table 1.

In general the shear stress is comprised of both the molecular and turbulent contributions, i.e., from Eqs. (12) and (13)

$$\tau' = -(\eta + \rho'\epsilon') \frac{d\bar{u}}{dy} \tag{16}$$

The present simple model of the turbulent flow structure also takes into account the observed increase in mass transfer. The appropriate phenomenological equation for material flux is given by

$$j = -(D_m + \epsilon'') \frac{dc}{dy} \tag{17}$$

where ϵ'' is the turbulent diffusivity. The von Karman similarity hypothesis postulates (*27*) that $\epsilon'' = \epsilon'$. Although experimental justification for this equivalence is not entirely conclusive, it appears reasonable (*24,26*) to assume

$$\epsilon'' = \epsilon' = \epsilon \tag{18}$$

for the present study.

Equations (12–17) and suitable expressions for ϵ in the region close to the wall serve now to relate the flow velocity and eddy viscosity. If empirical data on the dependence of either the ve-

locity or the eddy viscosity on the transverse coordinate are available, the others' dependence on this coordinate can be obtained via the above equations. Fortunately a wealth of experimental data has been gathered on velocity and eddy viscosity distributions (*24–34*) in the turbulent flow regions. It has become customary (*10,11,24–29*) to correlate all this data by the introduction of the dimensionless variables u_+ and y_+, defined by

$$u_+ = \frac{u}{u_*} \tag{19}$$

$$y_+ = \frac{u_*}{\nu} y \tag{20}$$

where

$$u_* = \sqrt{\frac{\tau_0'}{\rho'}} \tag{21}$$

and

$$\tau_0' = \frac{f\rho'\bar{u}}{2} \tag{22}$$

It has been argued (*10,11,26*) that u_+ is a single-valued function of y_+ in the turbulent flow region and there is overwhelming experimental support of this assumption for Re > 20,000 (*10,11,26,34*).

A number of studies (*10,11,24–26,28*) have established semi-empirical correlations relating ϵ/ν and u_+ to the dimensionless transverse coordinate y_+. It has also been shown (*10,11*) that the nature of these velocity profiles is determined mainly by the Reynolds number $2\bar{u}r_t/\nu$ and to a lesser extent by the Schmidt number, i.e., ν/Dm. For this reason most of the subsequent results will be cast in a dimensionless form. The main results of some of these studies are summarized in Table 1.

In the flow region 2000 < Re < 20,000 there appears to be some disagreement on the accuracy of the above-mentioned approach. Thus Sage et al. (*24,30*) have reported experimental evidence that u_+ and y_+ do not correlate the observed velocity distributions accurately enough in this region. Their observed velocity profiles are shown in Fig. 1. No attempt has been made to correlate this reported (*24,30*) deviation of $u_+(y_+)$ from a single-valued function in the flow region 3000 < Re < 20,000. To take this into account in the expressions for $u_+(y_+)$, an analytical expression was fitted very roughly to the few experimental results reported by Sage et al. For the region $0 \leq y_+ \leq 5$ it has been assumed that Eq. 23a

TABLE 1

Compilation of Some Expressions Proposed for u_+ and ϵ/ν

Region	u_+	ϵ/ν	Ref.
	Buffer Layer		
$0 \leqslant y_+ \leqslant 5$	y_+	1	von Karman (25)
$5 \leqslant y_+ \leqslant 30$	$-3.05 + 5.00 \ln y_+$	—	
$0 \leqslant y_+ \leqslant 5$	$u_+ = \frac{14.5}{3}\left[\frac{1}{2}\ln\frac{[1+(y_+/14.5)]^2}{1-(y_+/14.5)+(y_+/14.5)^2} + \sqrt{3}\tan^{-1}\frac{2y_+/14.5=1}{\sqrt{3}} + \frac{\pi\sqrt{3}}{6}\right]$ 23a	$(y_+/14.5)^3$	Lin (25)
$0 \leqslant y_+ \leqslant 33$	$-3.27 + 5 \ln (y_+ + 0.205)$	$(y_+/5) - 0.959$	Lin (25)
$0 \leqslant y_+ \leqslant 26$	$\int_0^y \frac{dy_+}{1 + 0.0154u_+y_+ [1 - \exp(-0.0154u_+y_+)]}$	$0.0154u_+y_+[1 - \exp(-0.0154u_+y_+)]$	Deissler (26)
$0 \leqslant y_+ \leqslant 27$	$\frac{1}{0.0695}\tanh(0.0695y_+)$	$\cosh^2(0.0695y_+) - 1$ 23b	Dunn (28)
	Turbulent core		
$y_+ \geqslant 30$	$5.5 + 2.5 \ln y_+$	$0.33y_+$	von Karman (25)
$y_+ \geqslant 27$	$3.8 + 2.8 \ln y_+$ 24a	$0.360y_+$ 24b	Deissler (26)

(see Table 1) still holds. In the region from $y_+ = 5$ to roughly $y_+ = 20$, the following expression was found to fit the experimental data suitably:

$$u_+ = 4.9 - \left[\frac{3.79 + 5.5z'}{\ln (6.6)}\right] \ln 5 + \left[\frac{3.79 + 5.5z'}{\ln (6.6)}\right] \ln y_+ \qquad (25)$$

z' is now a function of the Reynolds number and of the form

$$z' = 1 + 86700/\mathrm{Re}^{1.43} \qquad (26)$$

For the central core Eq. 24b (see Table 1) was modified to

$$u_+ = 3.8z' + 2.8 \ln y_+ \qquad (27)$$

In any subsequent calculations with Eqs. (25) and (27), the value of

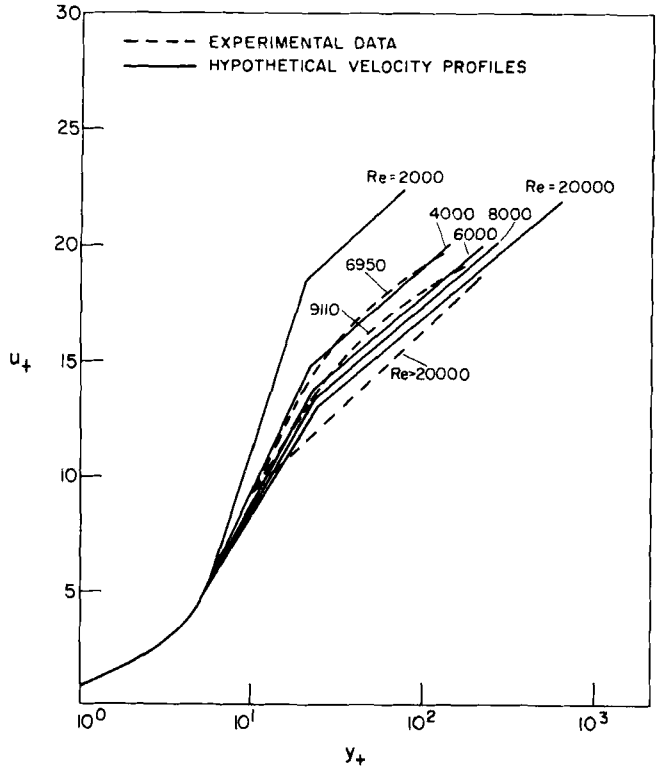

FIG. 1. Experimental evidence of the deviation of u_+ from a single-valued function of y_+ in the intermediate Reynolds number flow region.

y_+ at which both the equations yielded the same value of u_+ was determined from

$$u_+ \text{ [Eq. (25)]} = u_+ \text{ [Eq. (27)]}$$

This value depended only slightly on the Reynolds number and was ± 21.

The profiles calculated with the aid of Eqs. (25–27) are compared in Fig. 1 with the experimental data found by Sage et al. From this figure it is clear that the agreement between the experimental and the fitted curves is reasonable, and it would appear that the analytical expressions account satisfactorily for the relevant physical phenomena.

Finally ψ and ϕ can now be obtained directly from the semi-empirical functions $u_+(y_+)$ and $\epsilon(y_+)$ as follows. First, it follows from Eq. (17) that

$$D_r(r) = D_m + \epsilon = D_m \left(1 + \frac{\epsilon}{D_m}\right) \tag{28}$$

Clearly, from Eq. (4), if

$$D_r' = D_m$$

then

$$\psi(y_+) = 1 + \frac{\epsilon(y_+)}{D_m} \tag{29}$$

Second, taking Eq. (19) into consideration,

$$u(y_+) = u_* u_+ \tag{30}$$

After substitution of the empirical relation (11)

$$\tau_0' = 0.03325\rho'(\bar{u})^{7/4}\nu^{1/4}r_t^{-1/4} \tag{31}$$

into Eq. (21), it follows, upon rearrangement, that

$$u_* = 0.2\,\frac{\bar{u}}{\mathrm{Re}^{1/8}} \tag{32}$$

Thus from Eqs. (5), (30), and (32)

$$\phi(y_+) = \frac{0.2}{\mathrm{Re}^{1/8}}\,u_+ \tag{33}$$

EVALUATION OF THE PLATE HEIGHT FOR THE TURBULENT FLOW REGION

ϕ and ψ for the turbulent flow region are given by Eqs. (29) and (33) along with appropriate expressions for ϵ^+; and u_+. Before undertaking the actual evaluation of the plate, it is instructive to consider the variation of these quantities with the actual radial coordinate. In Fig. 2 the function $\phi(r_D)$ is shown. From this representation it is evident that the velocity profile becomes flatter and the laminar buffer layer narrower with increasing Reynolds number. Figure 3 depicts the dependence of ψ on $1 - r/r_t$. It is clear from this information that convective mechanisms contribute overwhelmingly to the dispersion coefficient near the center of the conduit and that this effect is more pronounced for liquids than for gases. The magnitude of this convective mechanism declines as the column wall is

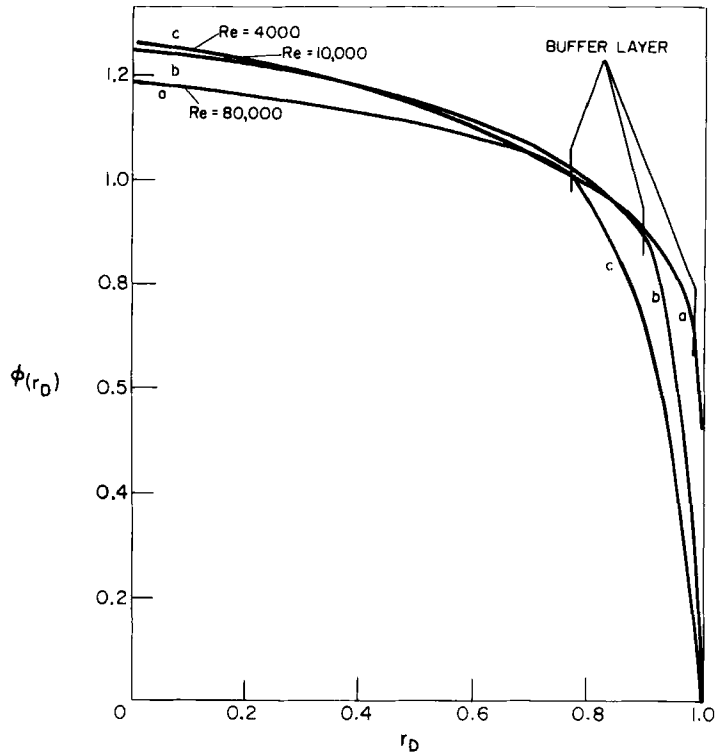

FIG. 2. Velocity profiles in the turbulent flow region.

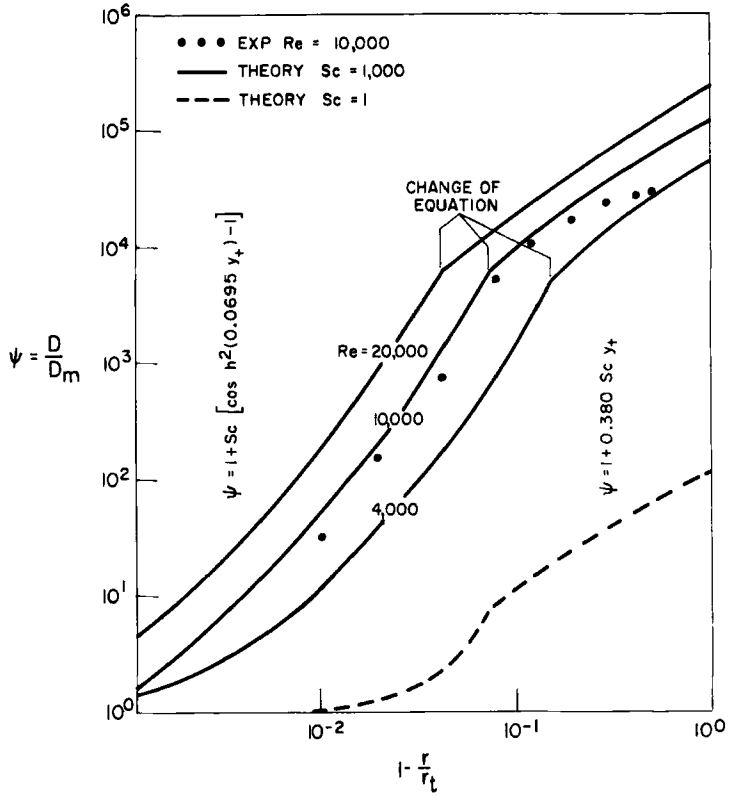

FIG. 3. Radial dependence of dispersion characteristics.

approached. Furthermore, convective mass-transport mechanisms are more significant closer to the wall for liquids than for gases. The experimental results (29) compare reasonably with the theoretical curves.

The integrals I_{11}, I_{12}, and I_{13} can now be rewritten in terms of the dimensionless quantities introduced above by employing the transformation

$$y_+ = g\left(1 - \frac{r}{r_t}\right) \tag{34}$$

where

$$g = 0.1\mathrm{Re}^{7/8} \tag{35}$$

It is thus found that

$$I_{11} = \int_o^g \frac{dy_+}{2(g - y_+)\psi(y_+)} \left[\int_{y_+}^g \frac{2[1 - (y_+/g)]\phi(y_+)\, dy_+}{g}\right]^2 \quad (36)$$

$$I_{12} = \int_o^g \frac{[1 - (y_+/g)]\, dy_+}{2g\psi(y_+)} \int_{y_+}^g \frac{2[1 - (y_+/g)]\phi(y_+)\, dy_+}{g} \quad (37)$$

$$I_{13} = \int_o^g \frac{[1 - (y_+/g)]^3\, dy_+}{2g\psi(y_+)} \quad (38)$$

The complexity of the expressions for these integrals frustrates any attempt to evaluate them analytically. Recourse has therefore had to be made to numerical integration by Newton–Cotes methods (35), and a Fortran IV program was written for an IBM 1130 digital computer to facilitate all the calculations.

Equations (36–38) were evaluated for the various proposed sets of phenomenological expressions summarized in Table 1. The agreement between the values of the integrals calculated for the various sets of expressions is reasonable. These values exhibit, furthermore, the same behavior in the range of Reynolds and Schmidt numbers considered. Only the integrals evaluated via the corrected velocity profiles, i.e., Eqs. (25–27) and Eqs. (23) and (24), are listed, together with $h_M(x)$ for $k = 0$, in Table 2 for various values of the Schmidt and Reynolds numbers. $h_M(x) = H_M(x)/r_t$, the reduced local plate height, is considered here and below to cover a wider range of parametric values.

It is interesting to note in Table 2 that the numerical values of the integrals I_{11}, I_{12}, and I_{13} are very nearly the same. Furthermore, for $k = 0$ the evaluation of the plate height with the aid of Eq. (1) and the data in Table 2 involves the difference of two very large quantities. This can best be illustrated by considering the case Sc = 1000 and Re = 10,000, where $(I_{11} - 2I_{12} + I_{13})$ ScRe = 22459 − 22452 = 7. Although reasonable care has been taken to obtain sufficient accuracy, discrepancies in these calculations can be expected and will have to be accepted as an inevitable consequence of plate-height expressions of this type. This numerical inaccuracy does not limit the present study seriously, since for values of k only slightly larger than zero ($k \geq 10^{-2}$), $I_{11}k^2$ becomes the dominant term in the plate-height expression. In this region the value of the plate height obtained from Eq. (1) and Table 2 depends almost solely on the value of I_{11} which is reliably known. This point is well demonstrated by considering Eq. (1) and Fig. 4.

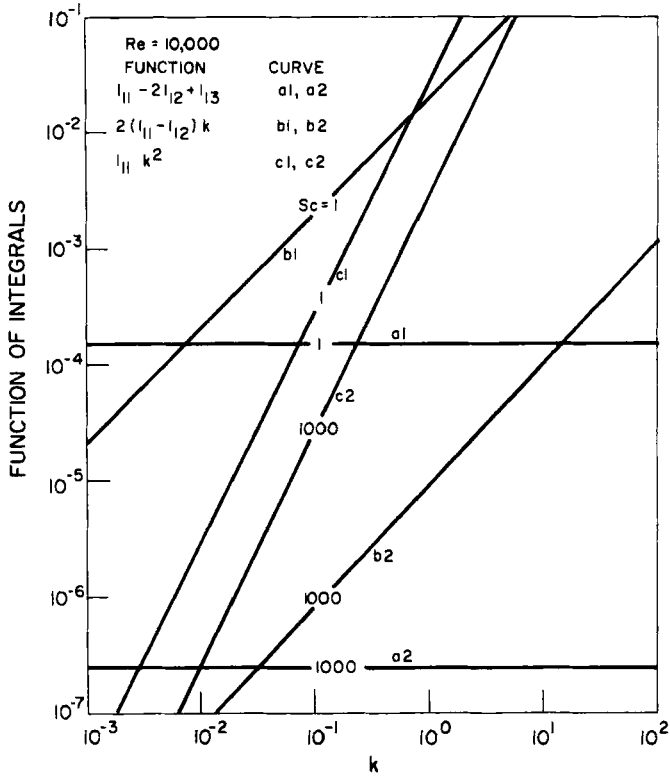

FIG. 4. Relative contributions of the respective terms to the value of $(I_{11} - 2I_{12} + I_{13}) + 2(I_{11} - I_{12})k + I_{11}k^2$.

This numerical form of the plate-height expression is inconvenient for subsequent use in calculations. The integrals in Table 2 were therefore used to obtain an analytical expression for $h_M(x)$ by numerically fitting them to suitable functions. These equations have been fitted to the data in the region $2300 < \mathrm{Re} < 100{,}000$. Thus for $\mathrm{Sc} = 1$

$$h_M(x) = \left[\frac{3.7810^4}{\mathrm{Re}^{2.1}} + 1.4 \times 10^{-5} + \left(\frac{218}{\mathrm{Re}^{1.19}} + 2.5910^{-5}\right) k + \left(\frac{46.01}{\mathrm{Re}^{0.81}} + 6.7 \times 10^{-4}\right) k^2\right] \frac{\mathrm{ScRe}}{(1+k)^2} \quad (39)$$

and for $\mathrm{Sc} = 1000$

$$h_M(x) = \left[\frac{36.01}{\mathrm{Re}^{1.89}} + 3.2 \times 10^{-8} + \left(\frac{3.70}{\mathrm{Re}^{1.18}} - 1.6 \times 10^{-6}\right) k + \left(\frac{27.55}{\mathrm{Re}^{1.11}} + 1 \times 10^{-4}\right) k^2\right] \frac{\mathrm{ScRe}}{(1+k)^2} \quad (40)$$

Equations (39) and (40) hold only for discrete Schmidt numbers. Although it should be possible to fit $h_M(x)$ numerically to two simultaneous variables, the resulting expressions are unwieldy. A simple expression that incorporates all the essential features of the

TABLE 2

Integrals I_{11}, I_{12}, and I_{13} Calculated with Modified Velocity Profiles [Eq. (25)][a]

Re	I_{11}	I_{12}	I_{13}	$h_M(x)$
		Sc = 1		
4,000	5.7643×10^{-2}	4.9839×10^{-2}	4.3210×10^{-2}	4.70
8,000	3.1759×10^{-2}	2.9438×10^{-2}	2.7331×10^{-2}	1.72
10,000	2.6680×10^{-2}	2.4978×10^{-2}	2.3420×10^{-2}	1.43
20,000	1.5796×10^{-2}	1.5013×10^{-2}	1.4285×10^{-2}	1.10
40,000	9.3527×10^{-3}	8.9529×10^{-3}	8.5779×10^{-3}	1.00
80,000	5.4674×10^{-3}	5.2772×10^{-3}	5.0973×10^{-3}	0.83
		Sc = 10		
4,000	2.3874×10^{-2}	2.1347×10^{-2}	1.9120×10^{-2}	12.04
8,000	1.2295×10^{-2}	1.1683×10^{-2}	1.1112×10^{-2}	3.21
10,000	1.0118×10^{-2}	9.6925×10^{-3}	9.2914×10^{-3}	2.48
20,000	5.6374×10^{-3}	5.4566×10^{-3}	5.2842×10^{-3}	1.68
40,000	3.1557×10^{-3}	3.0662×10^{-3}	2.9804×10^{-3}	1.46
80,000	1.7512×10^{-3}	1.7115×10^{-3}	1.6733×10^{-3}	1.12
		Sc = 100		
4,000	8.4755×10^{-3}	8.4755×10^{-3}	7.1350×10^{-3}	26.00
8,000	4.2865×10^{-3}	4.2865×10^{-3}	3.9986×10^{-3}	5.37
10,000	3.5079×10^{-3}	3.5079×10^{-3}	3.3115×10^{-3}	3.96
20,000	1.9215×10^{-3}	1.8779×10^{-3}	1.8355×10^{-3}	2.70
40,000	1.0581×10^{-3}	1.0353×10^{-3}	1.0131×10^{-3}	2.51
80,000	5.775×10^{-4}	5.6771×10^{-4}	5.5791×10^{-4}	1.87
		Sc = 1000		
4,000	2.7859×10^{-3}	2.5940×10^{-3}	2.4163×10^{-3}	56.91
8,000	1.4032×10^{-3}	1.3672×10^{-3}	1.3224×10^{-3}	9.19
10,000	1.1468×10^{-3}	1.1226×10^{-3}	1.0991×10^{-3}	6.56
20,000	6.2544×10^{-4}	6.1418×10^{-4}	6.0316×10^{-4}	4.93
40,000	3.4281×10^{-4}	3.3650×10^{-4}	3.3032×10^{-4}	5.27
80,000	1.8625×10^{-4}	1.8342×10^{-4}	1.8065×10^{-4}	3.94

[a] $h_M(x)$ for the case $k = 0$.

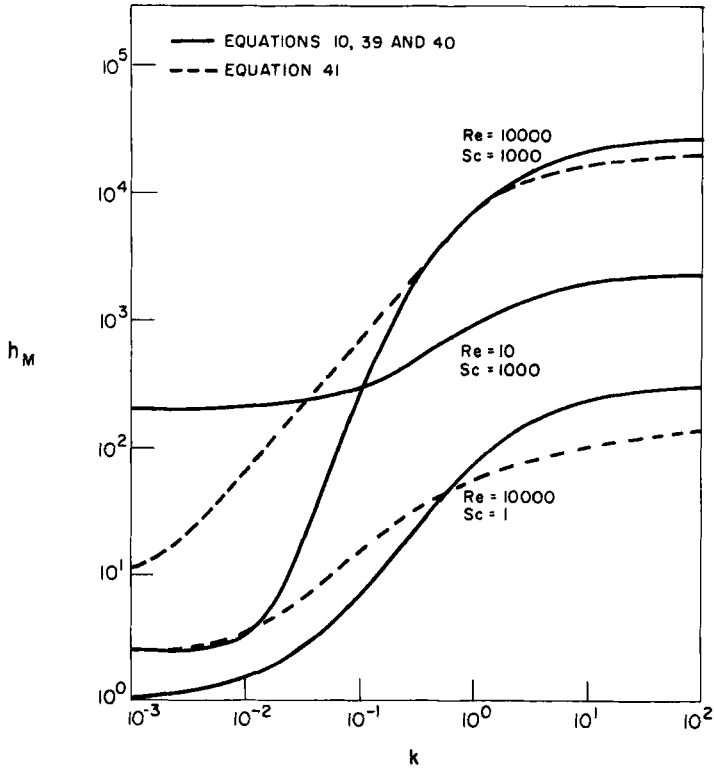

FIG. 5. Typical trends with k for both the laminar and turbulent flow regions.

more exact equation to a logarithmic degree of accuracy is

$$h_M(x) = \frac{36 \times 10^3}{(1+k)^2 \mathrm{Re}} + \frac{100 k \mathrm{Sc}^{2/3}}{(1+k)} \tag{41}$$

Equations (10) and (39–41) have been used to calculate the curves shown in Figs. 5 and 6. In the case of Eq. (10), $h_M(x)$ was obtained for the laminar flow region after rearrangement and by taking $C_s = 0$ and $p = 1$. The broken lines represent the approximate expression, Eq. (41).

DISCUSSION OF THE LOCAL PLATE HEIGHT FOR OPEN TUBULAR COLUMNS FOR $C_s = 0$

The well-known (*36–41*) behavior of $h_M(x)$ in the vicinity of its minimum ($\mathrm{ReSc} \simeq 2/\sqrt{I_1}$) in the laminar flow region is not shown

in Fig. 6 since the characteristics of the local plate height in the laminar region have been studied in great detail both experimentally and theoretically (*37–46*). The minimum of the plate height results from the competition between two band-broadening effects. On the one hand, at flow velocities that are too low, the solute band moves slowly enough for molecular diffusion to broaden the band significantly per unit distance traveled along the column. On the other hand, with increasing flow velocity, resistance to lateral mass transfer in the mobile phase contributes increasingly to the local plate height. The resulting minimum of $h_M(x)$ $[h_M(x) = 4\sqrt{I_1}]$ depends on the mass distribution coefficient k. For $k = 0$, $[h_M(x)]_{min} = 1/\sqrt{3}$. This value increases with k Thus when $k \to \infty$, $[h_M(x)]_{min} \simeq \sqrt{11/3}$. This represents an increase of about a factor of 3. In the higher Reynolds number region, shown in Fig. 6, $h_M(x)$

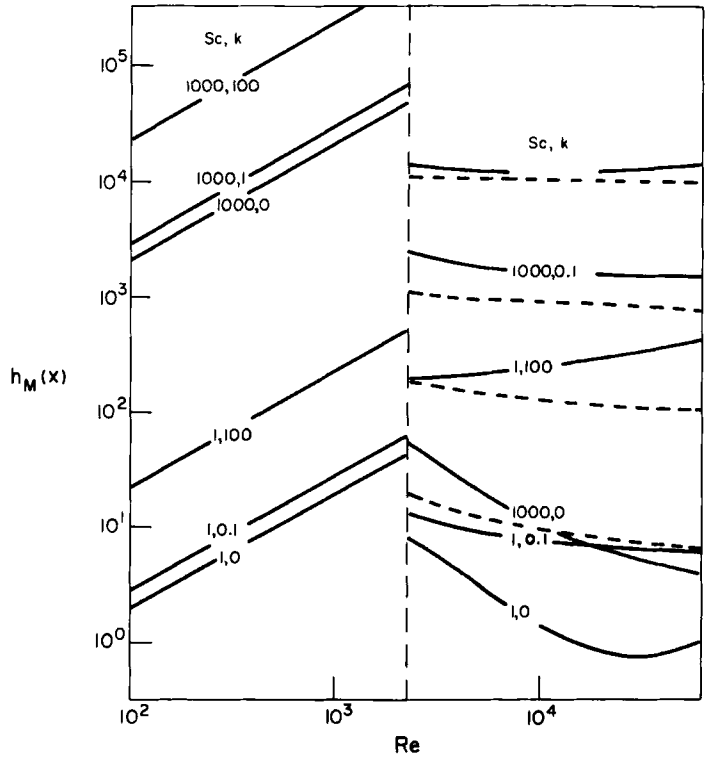

FIG. 6. Various significant trends in the reduced plate height in both the laminar and turbulent flow regions.

increases linearly with Re. In this region $h_M(x)$ changes by about a factor of 11 for a variation of k from 0 to large values (≥ 10). The variation of $h_M(x)$ with k is shown in Fig. 5. The linear increase can be expected to persist with increasing Reynolds number as long as the flow dynamics remain laminar. This Reynolds number range extends up to Re $\sim$ 2000.

As soon as turbulence sets in, the behavior of the local plate height with respect to changes in both Re and k becomes quite different from that in the laminar flow region. First, a pronounced decrease in $h_M(x)$ is observed as soon as the flow becomes turbulent. This decrease in $h_M(x)$ is much larger in the case of liquids (Sc $\simeq$ 1000) than in the case of gases (Sc $\simeq$ 1). Thus for liquids the predicted decrease in h_M for $k = 0$, when going from Re $\simeq 10^3$ to Re $\simeq 10^4$, is approximately five orders of magnitude. Furthermore, $h_M(x)$ in the turbulent flow region for $k = 0$ is of the same order of magnitude as its value at the optimum Reynolds number in the laminar flow region. Second, the increase of $h_M(x)$ with a large increment of k from $k = 0$ is much greater than in the laminar flow region. Here again, this effect is more pronounced for liquids than for gases, as is clearly demonstrated in Fig. 5 by the curves for Re = 10,000. In advance it may be expected that this trend of $h_M(x)$ may seriously limit the application of turbulent flow chromatography. Although there is a significant decrease in the plate height when turbulent rather than laminar flow is employed, the resultant value of $h_M(x)$ is still very large. From the point of view of separation time, however, the gain may still be worth further consideration.

The interpretation of the decrease of the local plate height in the turbulent flow region is, at this stage, obviously related to the enhanced lateral mass-transfer rates and flatter velocity profiles typical of turbulent flow dynamics. The unexpected k dependence of $h_M(x)$ in the turbulent flow region necessitates, however, more careful consideration. In this regard it should be pointed out that even for a flat velocity profile $h_M(x) > 0$ when $k > 0$, as can easily be verified from Eqs. (2–5). Thus for a hypothetical flat profile and $D_r(r) = D_m$, it follows for $k > 0$ that

$$h_M = \frac{1}{8} \frac{k^2}{(1+k)^2} \text{ReSc} \tag{42}$$

This band broadening results because solute molecules near the column wall have a greater chance of entering the stationary phase

than those further away and are thus transported at a rate slower than the average flow velocity (22). It has also been shown by de Clerk (7) that this mechanism is formally equivalent to a "virtual" velocity profile. Although it is not possible to distinguish quantitatively in the expressions for the plate height between contributions associated with "real" and those associated with "virtual" velocity profiles, consideration of Eq. (42) indicates that the effect of the virtual velocity profile manifests itself mainly in the coefficient of k^2 in the expression for h, i.e., with I_{11}. Furthermore, it is clear from Fig. 4 that it is mainly the $I_{11}k^2$ term that dominates the value of I_1, hence $h_M(x)$, at relatively large values of k. It is thus not unreasonable to conclude that it is mainly the effect of the virtual velocity profile that causes the undue band spreading at large k values. The absence of eddies in the laminar layer adjacent to the column wall and the high linear velocity of the turbulent core are physically responsible for the magnitude of this effect. The importance of the boundary layer properties is also accentuated by the difference in the values of $h_M(x)$ for gases and liquids when $k > 1$, as is evident from Fig. 5, if it is borne in mind that apart from the boundary layer these fluids exhibit largely the same properties in the turbulent flow region.

List of Symbols*

C_s	convenient parameter, related to the band-broadening mechanism residing in the stationary phase, defined by Eq. (1) (T)
c	concentration of solute in the mobile phase (ML^{-3})
D	dispersion coefficient (L^2T^{-1})
D_m	molecular diffusion coefficient in the mobile phase (L^2T^{-1})
D_{mo}	value of D_m measured at the column outlet (L^2T^{-1})
D_l	longitudinal dispersion coefficient (L^2T^{-1})
D_r	radial dispersion coefficient (L^2T^{-1})
D'_r	reference value of D_r, defined by Eq. (4) (L^2T^{-1})
D'_{ro}	value of D'_r measured at the column outlet (L^2T^{-1})
f	Fanning friction factor

* Dimensions are given where applicable in terms of mass (M), length (L), and time (T).

f_m	correction for compressibility of the mobile phase, given by Eq. (6)
f_s	correction for compressibility of the mobile phase, given by Eq. (7)
g	convenient parameter, defined by Eq. (35)
H	plate height measured at the column outlet (L)
H_M	contribution to H of the band-broadening mechanisms residing in the mobile phase (L)
$h = H/r_t$	reduced plate height
$h_M = H_M/r_t$	H_M measured in units of r_t
I_1	integral, defined by Eq. (2)
I_{11}, I_{12}, I_{13}	integrals, defined by Eq. (2)
j	material flux in the x direction, defined by Eq. (17) ($ML^{-2}T^{-1}$)
k	mass distribution coefficient; ratio of the solute mass in the stationary phase to the solute mass in the mobile phase at equilibrium
l	mixing length, defined by Eq. (14) (L)
P	pressure ($ML^{-1}T^{-2}$)
$p = P_i/P_o$	ratio of the inlet to the outlet pressure
Re	Reynolds number; $\mathrm{Re} = 2r_t\bar{u}(x)/\nu(x)$
r	radial coordinate (L)
$r_D = r/r_t$	dimensionless radial coordinate
r_t	radius of open tubular column (L)
$\mathrm{Sc} = \nu/D_m$	Schmidt number
u	linear flow velocity of the mobile phase in the axial direction (LT^{-1})
$\bar{u}$	radial average of u (LT^{-1})
$\bar{u}_o$	value of $\bar{u}$ measured at the column outlet (LT^{-1})
u'	velocity component of a macroscopic fluid element in the x direction (LT^{-1})
u''	component of turbulent fluctuation velocity of a macroscopic fluid element in the axial direction (LT^{-1})
$\bar{u}'$	temporal average of linear velocity of a macroscopic fluid element in the x direction (LT^{-1})
$u_+ = u/u_*$	dimensionless variable employed to correlate the velocity distribution $u(y)$ as a single-valued function in the turbulent flow region; see Eqs. (19–22)
$u_* = (\tau_0'/\rho')^{1/2}$	variable, defined by Eq. (21) (LT^{-1})

v' velocity component of a macroscopic fluid element in the y direction (LT^{-1})

$\bar{v}'$ temporal average of the linear velocity of a macroscopic fluid element in the y direction (LT^{-1})

v'' component of turbulent fluctuation velocity of a macroscopic fluid element in the y direction (LT^{-1})

w' velocity component of a macroscopic fluid element in the z direction (LT^{-1})

$\bar{w}'$ temporal average of linear velocity of a macroscopic fluid element in the z direction (LT^{-1})

w'' component of turbulent fluctuation velocity of a macroscopic fluid element in the z direction (LT^{-1})

y lateral y coordinate (L)

$y_+ = (u_*/\nu)y$ dimensionless variable employed to correlate the velocity distribution $u(y)$ as a single-valued function in the turbulent flow region; see Eq. (19–22)

z lateral z coordinate (L)

z' correction to velocity distribution $u_+(y_+)$, defined by Eq. (26)

ϵ symbol for turbulent viscosity as well as for turbulent diffusivity when these quantities are numerically equal (L^2T^{-1})

ϵ' virtual kinematic viscosity for turbulent flow, defined by Eq. (12) (L^2T^{-1})

ϵ'' virtual turbulent diffusivity, defined by Eq. (17) (L^2T^{-1})

η viscosity in the mobile phase ($ML^{-1}T^{-1}$)

κ empirical constant, defined by Eq. (14)

ν kinematic viscosity coefficient of the mobile phase

ρ' density of the mobile phase (ML^{-3})

τ_t' shear stress in the turbulent flow region, defined by Eq. (12) ($ML^{-1}T^{-2}$)

τ' shear stress in the absence of turbulence, defined by Eq. (13) ($ML^{-1}T^{-2}$)

τ_0' shear stress at the tube wall, given by Eq. (22) ($ML^{-1}T^{-2}$)

Φ integral, defined by Eq. (3)

ϕ function, indicative of the lateral variation in the linear velocity u, defined by Eq. (5)

ψ function, indicative of the lateral variation in the radial dispersion coefficient, defined by Eq. (4)

REFERENCES

1. V. Pretorius and T. W. Smuts, *Anal. Chem.*, **38**, 274 (1966).
2. J. C. Giddings, W. A. Manwaring, and M. N. Myers, *Science*, **154**, 146 (1966).
3. J. C. Sternberg and R. E. Poulson, *Anal. Chem.*, **36**, 1492 (1964).
4. J. C. Giddings, in *Dynamics of Chromatography*, Part I (J. C. Giddings and R. A. Keller, eds.), Dekker, New York, 1965.
5. T. W. Smuts, D. Sc. thesis, University of Pretoria, Pretoria, S. Africa, 1967.
6. G. I. Taylor, *Proc. Roy. Soc. (London)*, **A223**, 446 (1954).
7. K. de Clerk, D.Sc. thesis, University of Pretoria, Pretoria, S. Africa, 1966.
8. P. C. Haarhoff, D.Sc. thesis, University of Pretoria, Pretoria, S. Africa, 1962.
9. J. C. Giddings, S. L. Seager, L. R. Stucki, and G. H. Steward, *Anal. Chem.*, **32**, 867 (1960).
10. V. G. Levich, *Physicochemical Hydrodynamics*, Prentice-Hall, Englewood Cliffs, N.J., 1962.
11. H. Schlichting, *Boundary Layer Theory*, McGraw-Hill, New York, 1955.
12. A. A. Townsend, *The Structure of Turbulent Shear Flow*, New York, Cambridge Univ. Press, 1956.
13. J. O. Hinze, *Turbulence*, McGraw-Hill, New York, 1959.
14. V. L. Streeter, *Fluid Mechanics*, McGraw-Hill, New York, 1966.
15. L. D. Landau and E. M. Lifshitz, *Fluid Mechanics*, Pergamon Press, New York, 1959.
16. O. Reynolds, *Trans. Roy. Soc. London*, **174** (1883).
17. G. I. Taylor, *Proc. Roy. Soc. (London)*, **A151**, 421 (1935).
18. C. C. Lin, *Statistical Theories of Turbulence*, Princeton Univ. Press, Princeton, N.J., 1961.
19. L. Prandtl, *Essentials of Fluid Dynamics*, Hofner, New York, 1952.
20. G. B. Schubauer and C. M. Tchen, *Turbulent Flow*, Princeton Univ. Press, Princeton, N.J., 1961.
21. T. von Karman, *J. Marine Res.*, **7**, 252 (1948).
22. R. B. Bird, W. E. Steward, and E. N. Lightfoot, *Transport Phenomena*, Wiley, New York, 1960.
23. T. von Karman, *J. Aeron. Sci.*, **1**, 1 (1934).
24. J. B. Opfell and B. H. Sage, *Advan. Chem. Eng.*, **1**, 242 (1956).
25. C. S. Lin, R. W. Moulton, and G. L. Rutnam, *Ind. Eng. Chem.*, **45**, 636 (1953).
26. R. G. Deissler, in *Recent Advances in Heat and Mass Transfer* (J. P. Hartnett, ed.), McGraw-Hill, New York, 1961, p. 253.
27. T. von Karman, *Nachr. Akad. Wiss. Gottingen, Math.-Physik. Kl.* (1930).
28. L. G. Dunn, W. B. Powell, and H. S. Seifert, *3rd Anglo-American Aeronautical Conference*, Brighton, England, 1951.
29. W. H. Corcoran, J. B. Opfell, and B. H. Sage, *Momentum Transfer in Fluids*, Academic Press, New York, 1956.

30. W. G. Schlinger, V. J. Berry, J. L. Mason, and B. H. Sage, *Ind. Eng. Chem.*, **45,** 662 (1953).
31. R. C. Seagrave, *A.I.Ch.E.J.*, **11,** 748 (1965).
32. R. S. Brockly, *A.I.Ch.E.J.*, **12,** 403 (1966).
33. G. Q. Martin and L. N. Johanson, *A.I.Ch.E.J.*, **11,** 29 (1965).
34. J. Nikuradse, *VDI-Forschungsh.*, **356,** 1 (1932).
35. H. Margenau and G. M. Murphy, *The Mathematics of Physics and Chemistry,* Van Nostrand, Princeton, N.J., 1962.
36. L. S. Ettre, *Open Tubular Columns in Gas Chromatography,* Plenum Press, New York, 1965.
37. M. J. E. Golay, in *Gas Chromatography* (V. J. Coates, H. J. Noebels, I. S. Fagerson, eds.), Academic Press, New York, 1958.
38. P. C. Haarhoff and V. Pretorius, *J. S. African Chem. Inst.*, **13,** 97 (1960).
39. P. C. Haarhoff and V. Pretorius, *J. S. African Chem. Inst.*, **13,** 116 (1960).
40. M. J. E. Golay, *Nature,* **199,** 370 (1963).
41. R. Kaiser and H. G. Struppe, in *Gas Chromatography 1959, Second Symposium on Gas Chromatography* (R. E. Kaiser and H. G. Struppe, eds.), Böhler, 1959
42. R. P. W. Scott, *Nature,* **185,** 312 (1960).
43. D. H. Desty, A. Goldup, and B. H. F. Whyman, *J. Inst. Petrol.*, **45,** 287 (1959).
44. D. H. Desty, A. Goldup, and W. T. Swanton, *Nature,* **183,** 107 (1959).
45. D. H. Desty, A. Goldup, and W. T. Swanton, in *Third International Gas Chromatography Symposium* (H. Brenner, J. E. Callen, and M. D. Weiss, eds.), Academic Press, New York, 1962.
46. D. Jantzsch, G. Oesterhelt, E. Rodel, and H. G. Zimmermann, *Z. Anal. Chem.*, **205,** 237 (1964).

Received by editor November 27, 1967
Submitted for publication December 27, 1967